

Physiological Research Pre-Press Article

Effects of pioglitazone on ventricular myocyte shortening and Ca²⁺ transport in the Goto-Kakizaki type 2 diabetic rat

Salem KA – Department of Pharmacology, College of Medicine & Health Sciences UAE University, Al Ain, UAE. E-mail: khawla.abdulla@hotmail.com (PhD)

Sydorenko V - Department of Cellular Membranology³, Bogomoletz Institute of Physiology, Kiev, Ukraine. E-mail: vadym.sydorenko@gmail.com (PhD)

Qureshi MA – Department of Physiology, College of Medicine & Health Sciences UAE University, Al Ain, UAE. E-mail: anwar.queshi@uaeu.ac.ae (MSc)

Oz M – Department of Pharmacology, College of Medicine & Health Sciences UAE University, Al Ain, UAE. E-mail: Murat_Oz@uaeu.ac.ae (PhD)

Howarth FC - Department of Physiology, College of Medicine & Health Sciences UAE University, Al Ain, UAE. E-mail: chris.howarth@uaeu.ac.ae (PhD)

Address for correspondence:

Professor Chris Howarth
Department of Physiology
College of Medicine & Health Sciences
UAE University
P.O. Box 17666
Al Ain
UAE

Tel: 00 971 3 7137536
Fax: 00 971 3 7671966
Email: chris.howarth@uaeu.ac.ae

Summary

Pioglitazone (PIO) is a thiazolidindione antidiabetic agent which improves insulin sensitivity and reduces blood glucose in experimental animals and treated patients. At the cellular level the actions of PIO in diabetic heart are poorly understood. A previous study has demonstrated shortened action potential duration and inhibition of a variety of transmembrane currents including L-type Ca^{2+} current in normal canine ventricular myocytes. The effects of PIO on shortening and calcium transport in ventricular myocytes from the Goto-Kakizaki (GK) type 2 diabetic rat have been investigated. 10 min exposure to PIO (0.1-10 μM) reduced the amplitude of shortening to similar extents in ventricular myocytes from GK and control rats. 1 μM PIO reduced the amplitude of the Ca^{2+} transients to similar extents in ventricular myocytes from GK and control rats. Caffeine-induced Ca^{2+} release from the sarcoplasmic reticulum and recovery of Ca^{2+} transients following application of caffeine and myofilament sensitivity to Ca^{2+} were not significantly altered in ventricular myocytes from GK and control rats. Amplitude of L-type Ca^{2+} current was not significantly decreased in myocytes from GK compared to control rats and by PIO treatment. The negative inotropic effects of PIO may be attributed to a reduction in the amplitude of the Ca^{2+} transient however, the mechanisms remain to be resolved.

Keywords: Type 2 diabetes mellitus; Goto-Kakizaki rat; Ventricular myocytes; Calcium transport; Pioglitazone

Introduction

Diabetes mellitus (DM) is a debilitating disease that is estimated to affect 366 million people by 2030 worldwide. The risk of coronary heart disease is increased in patients with T2DM and cardiovascular disease causes 80% of all diabetic mortality and in 75% of cases, it is as a result of coronary atherosclerosis (Schwartz 2010). PIO belongs to the thiazolidinedione group of oral antidiabetic agents and is an agonist of peroxisome proliferator-activated receptor gamma (PPAR γ) (Yki-Jarvinen 2004). PIO decreases fasting and postprandial insulin concentrations and lowers blood pressure in spontaneously hypertensive rats (Grinsell *et al.* 2000). In the spontaneously obese, insulin-resistant rhesus monkey PIO improved fasting and postprandial levels of insulin sensitivity, plasma glucose and lipid levels and also decreased systolic and mean arterial pressure (Kemnitz *et al.* 1994). In a study to compare the risk of cardiovascular adverse effects in patients with T2DM treated with rosiglitazone, another thiazolidinedione, or PIO it was found that compared with pioglitazone, rosiglitazone is associated with an increased risk of myocardial infarction, heart failure, and all-cause mortality in diabetic patients (Nissen & Wolski 2007; Chen *et al.* 2012). High oral doses of PIO (500–1000 mg/kg) administered to mice produce hypertrophy of the heart and mild congestion of the liver and kidneys (Chinnam *et al.*, 2012). PIO attenuates congestive heart failure-induced atrial structural remodeling and atrial fibrillation in rabbit heart (Shimano *et al.* 2008). PIO has been shown to reduce angiotensin II-induced cardiac hypertrophy and ameliorate ventricular hypertrophy and fibrosis in hypertensive rat heart (Ye *et al.* 2005; Li *et al.* 2010; Kato *et al.* 2008). *In vivo* biotelemetry studies have reported that daily oral PIO administration at concentrations ranging from 2.5 to 20 mg/kg over a period of 14 weeks had no significant effects on heart rate, PQ and QT intervals and QRS

complex in GK rat hearts compared to controls (Salem *et al.* 2015). In primary cultured rat cardiac myocytes myocardial hypertrophy induced by glucose and insulin was inhibited by PIO (Liu *et al.* 2007). In canine ventricular myocytes action potential duration was shortened by PIO at concentrations $\geq 10 \mu\text{M}$ and this was accompanied by inhibition of several transmembrane ion currents including L-type Ca^{2+} current, the rapid and slow component of delayed rectifier K^{+} current and the transient outward K^{+} current (Kistamas *et al.* 2013). Little is known about the effect of PIO in diabetic heart. Therefore, the acute effects of PIO on ventricular myocyte shortening and Ca^{2+} transport have been investigated in GK type 2 diabetic rat.

Materials & Methods

Experimental protocol: Approval for this project was obtained from the Animal Ethics Committee, College of Medicine & Health Sciences, United Arab Emirates University.

Twelve male GK (Taconic, Germantown, NY, USA) and twelve male Wistar control rats aged 8-10 months were used in these experiments. Animals were supplied with standard rat chow and water *ad libitum*. Body weight, heart weight and non-fasting blood glucose were measured immediately prior to experiments.

Ventricular myocyte isolation: Left ventricular myocytes were isolated according to previously described techniques (Salem *et al.* 2013). In brief, animals were euthanized using a guillotine and hearts removed rapidly and mounted for retrograde perfusion according to the Langendorff method. Hearts were perfused at a constant flow rate of $8 \text{ ml.g heart}^{-1}.\text{min}^{-1}$ and at $36\text{-}37 \text{ }^{\circ}\text{C}$ with cell isolation solution containing in mM: 130.0 NaCl, 5.4 KCl, 1.4 MgCl_2 , 0.75 CaCl_2 , 0.4 NaH_2PO_4 , 5.0 HEPES, 10.0 glucose, 20.0 taurine and 10.0 creatine (pH 7.3). When the heart had

stabilized perfusion was switched for 4 min to Ca^{2+} - free cell isolation solution containing 0.1 mM EGTA, and then for 6 min to cell isolation solution containing 0.05 mM Ca^{2+} , 0.60 mg/ml type 1 collagenase (Worthington Biochemical Corp, Lakewood, NJ, USA) and 0.075 mg/ml type XIV protease (Sigma, Taufkirchen, Germany). Left ventricle tissue was excised from the heart, minced and gently shaken in collagenase-containing isolation solution supplemented with 1 % BSA. Cells were filtered from this solution at 4 min intervals and re-suspended in cell isolation solution containing 0.75 mM Ca^{2+} and stored at 4 °C.

Measurement of ventricular myocyte shortening: Ventricular myocyte shortening was measured according to previously described techniques (Salem *et al.* 2013). In brief, cells were allowed to settle on the glass bottom of a Perspex chamber mounted on the stage of an inverted microscope (Axiovert 35, Zeiss, Göttingen, Germany). Cells were superfused (3-5 ml/min) with normal Tyrode (NT) containing the following in mM: 140.0 NaCl, 5.0 KCl, 1.0 MgCl_2 , 10.0 glucose, 5.0 HEPES, 1.8 CaCl_2 (pH 7.4). Ventricular myocyte shortening was recorded using a video edge detection system (VED-114, Crystal Biotech, Northborough, MA, USA). Ventricular myocyte shortening was recorded before and after 10 min PIO treatment using a video edge detection system (VED-114, Crystal Biotech, Northborough, MA, USA). Superfusion of myocytes with NT and then NT + PIO were controlled by micropumps. Resting cell length, time to peak (TPK) shortening, time to half (THALF) relaxation and amplitude of shortening (expressed as a % of resting cell length) were measured in electrically stimulated (1 Hz) myocytes maintained at 35-36 °C before and after PIO. Myocytes with normal rod-shaped morphology and stable shortening during electrical stimulation were selected for experiments.

Data were acquired and analyzed with Signal Averager software v 6.37 (Cambridge Electronic Design, Cambridge, UK).

Measurement of intracellular Ca^{2+} transient: Myocytes were loaded with the fluorescent indicator fura-2 AM (F-1221, Molecular Probes, Eugene, OR, USA) according to previously described techniques (Salem *et al.* 2013). In brief, 6.25 μl of a 1.0 mM stock solution of fura-2 AM (dissolved in dimethylsulphoxide) was added to 2.5 ml of cells to give a final fura-2 concentration of 2.5 μM . Myocytes were shaken gently for 10 min at room temperature (24 °C). After loading with fura-2 AM, myocytes were centrifuged, washed with NT to remove extracellular fura-2 and then left for 30 min to ensure complete hydrolysis of the intracellular ester. To measure intracellular Ca^{2+} transients, myocytes were alternately illuminated by 340 nm and 380 nm light using a monochromator (Cairn Research, Faversham, UK) which changed the excitation light every 2 ms. The resulting fluorescence emitted at 510 nm was recorded by a photomultiplier tube and the ratio of the emitted fluorescence at the two excitation wavelengths (340/380 ratio) was calculated to provide an index of intracellular Ca^{2+} concentration. Resting fura-2 ratio, TPK Ca^{2+} transient, THALF decay of the Ca^{2+} transient and the amplitude of the Ca^{2+} transient (expressed as a percentage of a Ca^{2+} transient in Control and GK myocytes perfused with NT) were measured in electrically stimulated (1 Hz) myocytes maintained at 35-36 °C before and after PIO. Data were acquired and analyzed with Signal Averager software v 6.37 (Cambridge Electronic Design, Cambridge, UK).

Assessment of myofilament sensitivity to Ca^{2+} : In some cells shortening and fura-2 ratio were recorded simultaneously (Howarth *et al.* 2011). Myofilament sensitivity to Ca^{2+} was assessed from phase-plane diagrams of fura-2 ratio versus cell length by measuring the gradient of the

fura-2 - cell length trajectory during late relaxation of the twitch contraction before and after PIO. The position of the trajectory reflects the relative myofilament response to Ca^{2+} and hence, can be used as a measure of myofilament sensitivity to Ca^{2+} (Spurgeon *et al.* 1992; Howarth & Qureshi 2008).

Measurement of sarcoplasmic reticulum Ca^{2+} transport: Sarcoplasmic reticulum (SR) Ca^{2+} was assessed using previously described techniques (Howarth *et al.* 1999; Howarth *et al.* 2002; Bassani *et al.* 1995). After establishing steady state Ca^{2+} transients in electrically stimulated (1 Hz) myocytes maintained at 35-36 °C and loaded with fura-2, stimulation was paused for a period of 5 sec. Caffeine (20 mM) was then applied rapidly using a solution switching device (Levi *et al.* 1996). After 10 sec of caffeine, electrical stimulation was resumed and the Ca^{2+} transients were allowed to recover to steady state. SR releasable Ca^{2+} was assessed by measuring the amplitude of the caffeine-evoked Ca^{2+} transient. Refilling of SR was assessed by measuring the rate of recovery of electrically-evoked Ca^{2+} transients following application of caffeine. Measurements were made before and after PIO.

Measurement of L-type Ca^{2+} current: Voltage-dependent L-type Ca^{2+} current was measured selectively using whole-cell patch-clamp according to previously described techniques (Salem *et al.* 2013; Choi *et al.* 2002). L-type Ca^{2+} current was recorded with an Axopatch 200B amplifier (Molecular Devices, Sunnyvale, CA, USA). The analog signal was filtered using an eight-pole Bessel filter with a bandwidth of 5 kHz and digitized at a sampling rate of 10 kHz under software control (P Clamp 8.2, Molecular Devices, Sunnyvale, CA, USA). Patch pipettes were fabricated from filamented BF150-86-10 borosilicate glass (Sutter Instrument, CA, USA). The whole cell bath solution contained the following in mM: 145 NaCl, 2 MgCl_2 , 2 CaCl_2 , 10 HEPES and 10

glucose (pH 7.35). The pipette solution contained the following in mM: 140 CsCl, 2 MgCl₂, 10 TEA Cl, 10 EGTA, 10 HEPES, 1 MgATP (pH 7.25). Electrode resistances ranged from 3 to 5 MΩ, and seal resistances were 1–5 GΩ. Series resistances were compensated to >75 % of the uncompensated value. Experiments were performed at 34–36 °C before and after PIO. The current-voltage relationship was obtained by applying 300 ms test pulses in the range -60 mV to +70 mV in 10 mV steps from a holding potential of -50 mV. The steady-state inactivation of Ca²⁺ current was measured as the relationship of amplitude of the peak current at a test pulse of 0 mV to amplitude of peak current at 1000 ms long pre-pulses to various voltages between -60 and +30 mV. Normalized peak currents measured after these pre-pulses were plotted against the respective pre-pulse potential. Time course of recovery from inactivation was investigated using a two-pulse protocol. Two 100 ms depolarizing pulses to +10 mV were separated by inter-pulse intervals with variable duration. Peak Ca²⁺ current amplitude measured by the second pulse was normalized to that measured by the first pulse and their ratio was plotted against the inter-pulse interval. Data were acquired and analyzed with pClamp software v 8.2 (Axon Instruments Inc, Union City, CA, USA).

Drug preparation: PIO (E6910, Sigma-Aldrich) was dissolved in 100% DMSO to produce 50, 5 and 0.5 mM stock solutions which were stored at -20 °C. Experimental PIO solutions were prepared by addition of stock solutions to NT with final DMSO concentration of 0.02% in all test solutions.

Statistical analysis: Results are expressed as the mean ± SEM of ‘n’ observations. ‘n’ refers to number of animals or ventricular myocytes. Data were analyzed by the Independent samples t-

test, Paired samples t-test or as appropriate using IBM SPSS Statistics for Windows, Version 20.0 (IBM Corp, Armonk, NY). Statistical significance was set at $P < 0.05$

Results

Experiments were performed in cardiac myocytes isolated from GK rats, aged 8-10 months, and age-matched controls. Body weight, heart weight and non-fasting blood glucose were measured immediately before experiments. The results are shown in Table 1. Body weight and heart weight were significantly ($P < 0.01$) higher in GK compared to control rats. Non-fasting blood glucose was significantly ($P < 0.01$) elevated in GK compared to control rats. Heart weight to body weight ratio was not significantly ($P > 0.05$) altered in GK compared to control rats.

Table 1 - General characteristics of Goto-Kakizaki rats

	Control	GK
Bodyweight(g)	352.5 ± 11.6	417.83 ± 5.1**
Heart weight(g)	1.2 ± 0.03	1.4 ± 0.02**
Heart weight/body weight (mg/g)	3.4 ± 0.07	3.2 ± 0.03
Blood glucose(mg/dl)	96.9 ± 2.1	131.5 ± 3.6**

** $P < 0.01$, n=12 rats

Effects of acute Pioglitazone on ventricular myocyte shortening

Figure 1 shows the effects of different concentrations of PIO (0.1-10 μM) on the amplitude of myocyte shortening. Amplitude of shortening was significantly ($P < 0.05$) and progressively reduced in GK myocytes following treatment with 1 and 10 μM PIO and in control myocytes following treatment with 0.1, 1 and 10 μM PIO. 1 μM PIO was selected for further studies

because it produced a response intermediate between 0.1 and 10 μM and is considered a concentration that is clinically relevant (Budde *et al.* 2003). A typical recording of shortening in a GK myocyte superfused with NT or NT + 1 μM PIO is shown in Figure 2A. Resting cell length was not significantly ($P>0.05$) altered in GK myocytes compared to controls or by PIO (Fig. 2B). TPK shortening was significantly ($P<0.05$) prolonged in GK and control myocytes and THALF relaxation of shortening was significantly ($P<0.05$) prolonged only in GK myocytes with 1 μM PIO (Figs 2C, D). Amplitude of shortening was unaltered in GK myocytes compared to controls, PIO significantly ($P<0.05$) reduced amplitude of shortening in GK ($80.2\pm 2.7\%$, $n=24$) and control ($83.84 \pm 3.16\%$, $n=22$) myocytes (Fig. 2E).

Effects of acute Pioglitazone on ventricular myocyte intracellular Ca^{2+} transient

A typical recording of Ca^{2+} transient in a GK myocyte superfused with NT or NT + 1 μM PIO is shown in Figure 3A. Resting fura-2 ratio was not significantly ($P>0.05$) altered in GK or control myocytes or by PIO (Fig. 3B). TPK Ca^{2+} transient was prolonged by PIO in GK and control myocytes (Fig. 3C). THALF decay of the Ca^{2+} transient was significantly ($P<0.05$) shortened in GK compared to control myocytes (Fig. 3D). Amplitude of the Ca^{2+} transient was significantly ($P<0.05$) reduced in GK and control myocytes by PIO (Fig. 3E).

Effects of Pioglitazone on myofilament sensitivity to Ca^{2+}

In some experiments myocyte shortening and intracellular Ca^{2+} transient were recorded simultaneously. Typical records of myocyte shortening and fura-2 ratio in NT and a typical

phase plane diagram of fura-2 ratio vs. cell length in NT are shown in Figure 4A and B, respectively. The gradient of the fura-2 -cell length trajectory during late relaxation of the twitch contraction was not significantly ($P>0.05$) altered in GK compared to control myocytes or by PIO during the periods 500-800 ms (Fig. 4C), 500-700 ms (Fig. 4D) and 500-600 ms (Fig. 4E).

Effects of Pioglitazone on sarcoplasmic reticulum Ca^{2+} transport

The effects of PIO on SR Ca^{2+} were assessed in fura-2 loaded myocytes from GK and control rat. A typical record of the experimental protocol in a control myocyte is shown in Figure 5A. Caffeine-induced Ca^{2+} release from the SR was not significantly altered in GK compared to control myocytes or by PIO (Fig. 5B). Recovery of the Ca^{2+} transient following application of caffeine was not significantly ($P>0.05$) altered in GK compared to control myocytes or by PIO (Fig. 5C).

Effects of Pioglitazone on L-type Ca^{2+} current

The electrophysiological protocols (upper panel) that were used and typical current records of Ca^{2+} current in a control myocyte (lower panel) during activation, inactivation and restitution experiments are shown in Figure 6A, B and C, respectively. Over a range of test potentials the amplitude of L-type Ca^{2+} current was not significantly ($P>0.05$) reduced in GK compared to control myocytes or by PIO (Fig. 6D). At a test potential of 0 mV the amplitude of L-type Ca^{2+}

current was largest in control myocytes (7.4 ± 1.3 pA/pF, $n=11$), then control myocytes with PIO (6.1 ± 1.4 pA/pF, $n=9$), then GK myocytes (5.8 ± 0.9 pA/pF, $n=10$) and smallest in GK myocyte with PIO (5.0 ± 0.7 pA/pF, $n=9$) however, these differences were not significant ($P > 0.05$) (Fig. 6E). Inactivation of L-type Ca^{2+} current, was not significantly ($P > 0.05$) altered in GK compared to control myocytes or by PIO (Fig. 6F). Similarly, the time course of recovery from inactivation was not significantly ($P > 0.05$) altered in GK compared to control myocytes or by PIO (Fig. 6G).

Discussion

In recent years much of the research has focused on the potential effects of PIO on cardiovascular function. At the cellular level the actions of PIO in diabetic heart are poorly understood. The effects of PIO on ventricular myocyte shortening and Ca^{2+} transport have been investigated in this study. The major findings were: (1) PIO in the range 0.1-10 μM reduced the amplitude of shortening to similar extents in GK and control myocytes, (2) 1 μM PIO reduced the amplitude of the Ca^{2+} transient to similar extents in GK and control myocytes, (3) Myofilament sensitivity to Ca^{2+} was not altered in GK compared to control myocytes or by PIO, (4) Caffeine-induced Ca^{2+} release from the SR and recovery of the Ca^{2+} transients following application of caffeine was not significantly ($P > 0.05$) altered in GK compared to control myocytes or by PIO and (5) L-type Ca^{2+} current was not significantly altered in GK compared to control myocytes or by PIO.

Experiments were performed in GK rats, 8-10 months of age, and age-matched controls. Diabetes status was confirmed by elevated blood glucose, a finding that is consistent with

previous studies (Howarth *et al.* 2008). It has been reported that blood glucose is elevated from as young as 1 month in GK rats (Portha *et al.* 1991). Body weight was higher in GK rats compared to controls. PIO belongs to the thiazolidinedione group of oral antidiabetic agents, which act as full agonists of PPAR γ which is associated with glucose homeostasis (Willson *et al.* 1996; Zhang *et al.* 2007; Picard & Auwerx 2002; Gurnell *et al.* 2003). Many experimental and clinical studies have demonstrated the favorable effects of PIO on the modulation of cardiovascular risk factors related to T2DM (Lincoff *et al.* 2007; Dormandy *et al.* 2005; van der Meer *et al.* 2009; Kim *et al.* 2003; Rodriguez *et al.* 2006). Furthermore, previous studies have shown that the effects of PIO on the cardiovascular system are initiated at the pre-diabetes stage in type 2 diabetic rat (Tsuji *et al.* 2001). In this study 1 μ M PIO significantly reduced the amplitude and prolonged the TPK shortening in GK and control myocytes to similar extents. Resting cell length was not altered in GK compared to control myocytes or by PIO. In a previous study PIO treatment reduced cardiac cell length in myocytes from transgenic rats over expressing renin compared to non-transgenic littermates (Hinrichs *et al.* 2011). It's well known that Ca²⁺ is fundamental to the process of excitation-contraction coupling in cardiac muscle (Bers 2002). A previous study has shown that rosiglitazone was able to improve Ca²⁺ transport dysregulation in ventricular myocytes from streptozotocin-induced diabetic rat (Lee *et al.* 2013).

PIO decreased the amplitude and prolonged the TPK of the Ca²⁺ transient in GK and control myocytes. The effects of PIO on the Ca²⁺ transient may, at least in part, underlie the changes in shortening. Myofilament sensitivity to Ca²⁺ was assessed from phase-plane diagrams of fura-2 ratio vs. cell length by measuring the gradient of the fura-2-cell length trajectory during late relaxation of the twitch contraction (Spurgeon *et al.* 1992). The position of the trajectory reflects

the relative myofilament response to Ca^{2+} and hence, can be used as a measure of myofilament sensitivity to Ca^{2+} . Myofilament sensitivity to Ca^{2+} was not altered by PIO suggesting that the negative inotropic effects of PIO could not be attributed to altered myofilament sensitivity to Ca^{2+} . Release of Ca^{2+} from the SR during the process of excitation-contraction coupling contributes greatly to the generation of the Ca^{2+} transient in cardiac myocytes (Bers 2002). Therefore, SR Ca^{2+} transport was assessed before and after PIO treatment. Caffeine-evoked SR Ca^{2+} release was not altered in GK compared to control myocytes or by PIO. The recovery of the Ca^{2+} transient, following caffeine application and resumption of electrical stimulation, was not altered in GK myocytes compared to controls or by PIO suggesting that PIO does not affect SR Ca^{2+} release or reuptake. L-type Ca^{2+} current is the primary trigger for SR Ca^{2+} release. Amplitude of Ca^{2+} current was not significantly reduced in GK compared to control myocytes or by PIO. Previous studies in canine ventricular myocytes showed that several transmembrane ionic currents including L-type Ca^{2+} current were inhibited by $\geq 10 \mu\text{M}$ PIO (Kistamas *et al.* 2013). The $\text{Na}^+/\text{Ca}^{2+}$ exchange provides another transport system by which Ca^{2+} can enter or exit the cell and therefore influence the generation and/or the decay of the Ca^{2+} transient. A previous study in myocytes from streptozotocin - induced diabetic rat demonstrated depressed $\text{Na}^+/\text{Ca}^{2+}$ exchange (Choi *et al.* 2002). Further studies would be required to investigate the effects of PIO on $\text{Na}^+/\text{Ca}^{2+}$ exchanger in myocytes from GK rat.

In conclusion the negative inotropic effects of PIO in GK and control myocytes are similar and may partly be attributed to a reduction in Ca^{2+} transient however, the mechanisms remain to be resolved.

Acknowledgements: The work has been supported by a grant from the College of Medicine & Health Sciences, United Arab Emirates University. Research in our laboratory is also supported by LABCO, a partner of Sigma-Aldrich.

Competing interests: The author(s) declare(s) that they have no competing interests.

Authors contributions:

Salem KA was involved in the experiments, data analysis and in the preparation of the manuscript. Sydorenko V and Qureshi MA were involved in the experiments and data analysis. Oz M was involved in writing the manuscript. Howarth FC conceived of the study, secured grant funding, participated in its design and coordination and helped to draft the manuscript.

References

- BASSANI JW, YUAN WL, BERS DM: Fractional SR Ca release is regulated by trigger Ca and SR Ca content in cardiac myocytes. *Am J Physiol* **37**: C1313-C1319, 1995.
- BERS DM: Cardiac excitation-contraction coupling. *Nature* **415**,: 198-205, 2002.
- BUDDE K, NEUMAYER HH, FRITSCH L, SULOWICZ W, STOMPOR T, ECKLAND D: The pharmacokinetics of pioglitazone in patients with impaired renal function. *Br J Clin Pharmacol* **55**: 368-374, 2003.
- CHEN X, YANG L, ZHAI SD: Risk of cardiovascular disease and all-cause mortality among diabetic patients prescribed rosiglitazone or pioglitazone: a meta-analysis of retrospective cohort studies. *Chin Med J (Engl)* **125**: 4301-4306, 2012.
- CHINNAM P, MOHSIN M, & SHAFEE LM: Evaluation of acute toxicity of pioglitazone in mice. *Toxicol Int* **19**: 250-254, 2012.
- CHOI KM, ZHONG Y, HOIT BD, GRUPP IL, HAHN H, DILLY KW, GUATIMOSIM S, LEDERER WJ, MATLIB MA: Defective intracellular Ca(2+) signaling contributes to cardiomyopathy in Type 1 diabetic rats. *Am J Physiol* **283**: H1398-H1408, 2002.
- DORMANDY JA, CHARBONNEL B, ECKLAND DJ, ERDMANN E, MASSI-BENEDETTI M, MOULES IK, SKENE AM, TAN MH, LEFEBVRE PJ, MURRAY GD, STANDL E, WILCOX RG, WILHELMSSEN L, BETTERIDGE J, BIRKELAND K, GOLAY A, HEINA RJ, KORANYI L, LAAKSO M, MOKAN M, NORKUS A, PIRAGS V, PODAR T, SCHEEN A, SCHERBAUM W, SCHERNTHANER G, SCHMITZ O, SKRHA J, SMITH U, TATON J: Secondary prevention of macrovascular events in patients with type 2 diabetes in the PROactive Study (PROspective pioglitazone Clinical Trial In macroVascular Events): a randomised controlled trial. *Lancet* **366**: 1279-1289, 2005.
- GRINSELL JW, LARDINOIS CK, SWISLOCKI A, GONZALEZ R, SARE JS, MICHAELS JR, STARICH GH: Pioglitazone attenuates basal and postprandial insulin concentrations and blood pressure in the spontaneously hypertensive rat. *Am J Hypertens* **13**: 370-375, 2000.
- GURNELL M, SAVAGE DB, CHATTERJEE VK, O'RAHILLY S: The metabolic syndrome: peroxisome proliferator-activated receptor gamma and its therapeutic modulation. *J Clin Endocrinol Metab* **88**: 2412-2421, 2003.
- HINRICHS S, HEGER J, SCHRECKENBERG R, WENZEL S, EULER G, ARENS C, BADER M, ROSENKRANZ S, CAGLAYAN E, SCHLUTER KD: Controlling cardiomyocyte length: the role of renin and PPAR- γ . *Cardiovasc Res* **89**: 344-352, 2011.
- HOWARTH FC, CALAGHAN SC, BOYETT MR, WHITE E: Effect of the microtubule polymerizing agent taxol on contraction, Ca²⁺ transient and L-type Ca²⁺ current in rat ventricular myocytes. *J Physiol* **516**: 409-419, 1999.
- HOWARTH FC, JACOBSON M, SHAFIULLAH M, ADEGHATE E: Long-term effects of type 2 diabetes mellitus on heart rhythm in the Goto-Kakizaki rat. *Exp Physiol* **93**: 362-369, 2008.
- HOWARTH FC & QURESHI MA: Myofilament sensitivity to Ca²⁺ in ventricular myocytes from the Goto-Kakizaki diabetic rat. *Mol Cell Biochem* **315**: 69-74, 2008.
- HOWARTH FC, QURESHI MA, SOBHAY ZH, PAREKH K, YAMMAHI SR, ADRIAN TE, ADEGHATE E: Structural lesions and changing pattern of expression of genes encoding cardiac muscle proteins are associated with ventricular myocyte dysfunction in type 2 diabetic Goto-Kakizaki rats fed a high-fat diet. *Exp Physiol* **96**: 765-777, 2011.

HOWARTH FC, QURESHI MA, WHITE E: Effects of hyperosmotic shrinking on ventricular myocyte shortening and intracellular Ca(2+) in streptozotocin-induced diabetic rats. *Pflügers Arch* **444**: 446-451, 2002.

KATO MF, SHIBATA R, OBATA K, MIYACHI M, YAZAWA H, TSUBOI K, YAMADA T, NISHIZAWA T, NODA A, CHENG XW, MURATE T, KOIKE Y, MUROHARA T, YOKATA M, NAGATA K: Pioglitazone attenuates cardiac hypertrophy in rats with salt-sensitive hypertension: role of activation of AMP-activated protein kinase and inhibition of Akt. *J Hypertens* **26**: 1669-1676, 2008.

KEMNITZ JW, ELSON DF, ROECKER EB, BAUM ST, BERGMAN RN, MEGLASSON MD: Pioglitazone increases insulin sensitivity, reduces blood glucose, insulin, and lipid levels, and lowers blood pressure, in obese, insulin-resistant rhesus monkeys. *Diabetes* **43**: 204-211, 1994.

KIM SK, ZHAO ZS, LEE YJ, LEE KE, KANG SM, CHOI D, LIM SK, CHUNG N, LEE HC, CHA BS: Left-ventricular diastolic dysfunction may be prevented by chronic treatment with PPAR-alpha or -gamma agonists in a type 2 diabetic animal model. *Diabetes Metab Res Rev* **19**: 487-493, 2003.

KISTAMUS K, SZENTANDRASSY N, HEGYI B, RUZSNAVSZKY F, VACZI K, BARANDI L, HORVATH B, SZEKENI A, MAGYAR J, BANYASZ T, KECSKEMETI V, NANASI PP: Effects of pioglitazone on cardiac ion currents and action potential morphology in canine ventricular myocytes. *Eur J Pharmacol* **710**: 10-19, 2013.

LEE TI, CHEN YC, KAO YH, HSIAO FC, LIN YK, CHEN YJ: Rosiglitazone induces arrhythmogenesis in diabetic hypertensive rats with calcium handling alteration. *Int J Cardiol* **165**: 299-307, 2013.

LEVI AJ, HANCOX JC, HOWARTH FC, CROKER J, VINNICOMBE J: A method for making rapid changes of superfusate whilst maintaining temperature at 37 degrees C. *Pflügers Arch* **432**: 930-937, 1996.

LI P, SHIBATA R, UNNO K, SHIMANO M, FURUKAWA M, OHASHI T, CHENG X, NAGATA K, OUCHI N, MUROHARA T: Evidence for the importance of adiponectin in the cardioprotective effects of pioglitazone. *Hypertension* **55**: 69-75, 2010.

LINCOFF AM, WOLSKI K, NICHOLLS SJ, NISSEN SE: Pioglitazone and risk of cardiovascular events in patients with type 2 diabetes mellitus: a meta-analysis of randomized trials. *JAMA* **298**: 1180-1188, 2007.

LIU J, LIU Z, HUANG F, XING Z, WANG H, LI Z: Pioglitazone inhibits hypertrophy induced by high glucose and insulin in cultured neonatal rat cardiomyocytes. *Pharmazie* **62**: 925-929, 2007.

NISSEN SE & WOLSKI K: Effect of rosiglitazone on the risk of myocardial infarction and death from cardiovascular causes. *N Engl J Med* **356**: 2457-2471, 2007.

PICARD F & AUWERX J: PPAR(gamma) and glucose homeostasis. *Annu Rev Nutr* **22**: 167-197, 2002.

PORTHA B, SERRADAS P, BAILBE D, SUZUKI K, GOTO Y, GIROIX MH: Beta-cell insensitivity to glucose in the GK rat, a spontaneous nonobese model for type II diabetes. *Diabetes* **40**, 486-491, 1991.

RODRIGUEZ WE, JOSHUA IG, FALCONE JC, TYAGI SC: Pioglitazone prevents cardiac remodeling in high-fat, high-calorie-induced Type 2 diabetes mellitus. *Am J Physiol* **291**: H81-H87, 2006.

SALEM KA, JACOBSON M, SHAFIULLAH M, OZ M, ADEGHATE E, HOWARTH FC: Effects of pioglitazone on the electrocardiogram in the Goto-Kakizaki type 2 diabetic rat heart. *J Clin Exp Res Cardiol* **1[3]**: 301-306, 2015.

SALEM KA, QURESHI MA, SYDORENKO V, PAREKH K, JAYAPRAKASH P, IQBAL T, SINGH J, OZ M, ADRIAN TE, HOWARTH FC: Effects of exercise training on excitation-contraction coupling and related mRNA expression in hearts of Goto-Kakizaki type 2 diabetic rats. *Mol Cell Biochem* **380**: 83-96, 2013.

SCHWARTZ SS: Pioglitazone for the treatment of type 2 diabetes in patients inadequately controlled on insulin. *Diabetes Metab Syndr Obes* **3**: 243-252, 2010.

SHIMANO M, TSUJI Y, INDEN Y, KITAMURA K, UCHIKAWA T, HARATA S, NATTEL S, MUROHARA T: Pioglitazone, a peroxisome proliferator-activated receptor-gamma activator, attenuates atrial fibrosis and atrial fibrillation promotion in rabbits with congestive heart failure. *Heart Rhythm* **5**: 451-459, 2008.

SPURGEON HA, DUBELLI WH, STERN MD, SOLLOTT SJ, ZIMAN BD, SILVERMAN HS, CAPOGROSSI MC, TALO A, LAKATTA EG: Cytosolic calcium and myofilaments in single rat cardiac myocytes achieve a dynamic equilibrium during twitch relaxation. *J Physiol* **447**: 83-102, 1992.

TSUJI T, MIZUSHIGE K, NOMA T, MURAKAMI K, OHMORI K, MIYATAKE A, KOHNO M: Pioglitazone improves left ventricular diastolic function and decreases collagen accumulation in prediabetic stage of a type II diabetic rat. *J Cardiovasc Pharmacol* **38**: 868-874, 2001.

van der Meer RW, Rijzewijk LJ, de Jong HW, Lamb HJ, Lubberink M, Romijn JA, Bax JJ, de ROOS A, KAMP O, PAULUS WJ, HEINE RJ, LAMMERTSMA AA, SMIT JW, DIAMANT M: Pioglitazone improves cardiac function and alters myocardial substrate metabolism without affecting cardiac triglyceride accumulation and high-energy phosphate metabolism in patients with well-controlled type 2 diabetes mellitus. *Circulation* **119**: 2069-2077, 2009.

WILLSON TM, COBB JE, COWAN DJ, WIETHE RW, CORREA ID, PRAKASH SR, BECK KD, MOORE LB, KLIEWER SA, LEHMANN JM: The structure-activity relationship between peroxisome proliferator-activated receptor gamma agonism and the antihyperglycemic activity of thiazolidinediones. *J Med Chem* **39**: 665-668, 1996.

YE P, ZHANG C, WU SM, LIU YX: [Pioglitazone inhibits cardiac hypertrophy of rats in vitro and in vivo]. *Zhongguo Ying Yong Sheng Li Xue Za Zhi* **21**: 35-39, 2005.

YKI-JARVINEN H: Thiazolidinediones. *N Engl J Med* **351**: 1106-1118, 2004.

ZHANG F, LAVAN BE, GREGOIRE FM: Selective Modulators of PPAR-gamma Activity: Molecular Aspects Related to Obesity and Side-Effects. *PPAR Res* **2007**: 32696, 2007.

Figure legends

Figure 1

Effects of different concentrations of Pioglitazone (PIO) 0.1-10 μM on amplitude of ventricular myocyte shortening. Data are mean \pm SEM, n=14-19 cells from 9-10 hearts. Horizontal lines above graph bars illustrate significant difference ($P<0.05$).

Figure 2

Effects of Pioglitazone (PIO) on amplitude and time-course of ventricular myocyte shortening. A, Typical records of shortening in a GK myocyte superfused with either normal Tyrode (NT) or NT + 1 μM PIO. B, Resting cell length (RCL). C, Time to peak shortening. D, Time to half relaxation of shortening. E, amplitude of shortening. Data are mean \pm SEM, n=22-24 cells from 8 hearts. Horizontal lines above graph bars illustrate significant difference ($P<0.05$).

Figure 3

Effects of Pioglitazone (PIO) on Calcium transient of ventricular myocyte. A, Typical records of Ca^{2+} transient in a GK myocyte superfused with either normal Tyrode (NT) or NT+ 1 μM PIO. B, Resting fura-2 ratio. C, Time to peak Ca^{2+} transient. D, Time to half relaxation of Ca^{2+} transient. E, Amplitude of Ca^{2+} transient. Data are mean \pm SEM, n=20-24 cells from 8 hearts. Horizontal lines above graph bars illustrate significant difference ($P<0.05$).

Figure 4

Effects of Pioglitazone (PIO) myofilament sensitivity to Ca^{2+} of ventricular myocyte. A, Typical records of shortening and Ca^{2+} transient recorded simultaneously in a control myocyte superfused with either normal Tyrode (NT) or NT+ 1 μM PIO. B, Typical phase plane diagram of fura-2 ratio unit (RU) vs. cell length in a control myocyte. The solid arrow and bar in B indicate where the gradient was measured. Gradient of the fura-2-cell length trajectory during late relaxation of twitch contraction during the period (C), 500-800 ms. (D), 500-700 ms. (E), 500-600 ms. Data are mean \pm SEM, n=21-26 cells from 8 hearts.

Figure 5

Effects of Pioglitazone (PIO) on Sarcoplasmic reticulum (SR) Ca^{2+} transport of ventricular myocyte. A, Typical record of utilized protocol from control myocyte. B, Amplitude of caffeine-evoked Ca^{2+} transient. C, Recovery of the Ca^{2+} transient following rapid application of caffeine. Data are mean \pm SEM, n=25-36 cells from 10 hearts. Horizontal lines above graph bars illustrate significant difference ($P < 0.05$).

Figure 6

Effects of Pioglitazone (PIO) on amplitude of L-type Ca^{2+} current. Voltage protocols (upper panel) and typical records (lower panel) of A, Activation. B, Inactivation. C, Restitution of L-type Ca^{2+} current in a control myocyte. D, Activation current at voltages ranging from -60 to +70

mV. E, Mean L-type Ca^{2+} current evoked by test potentials to 0 mV. F, Inactivation curve at pre-pulse voltage ranging from -60 to +30 mV. G, Restitution curve at inter-pulse timing ranging from 25 to 70 ms. Data are mean \pm SEM, n = 9-11 cells from 4-6 hearts.

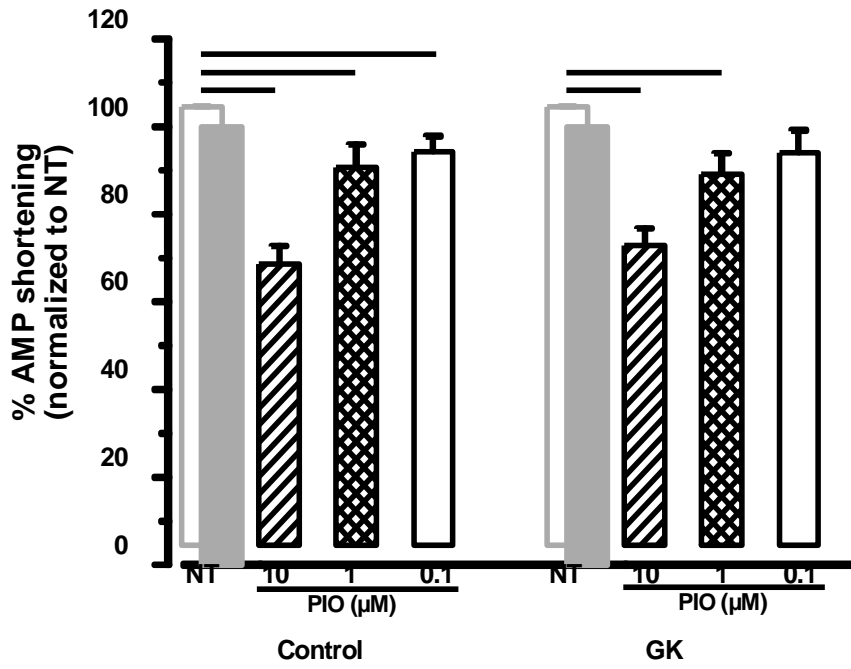


Figure 1

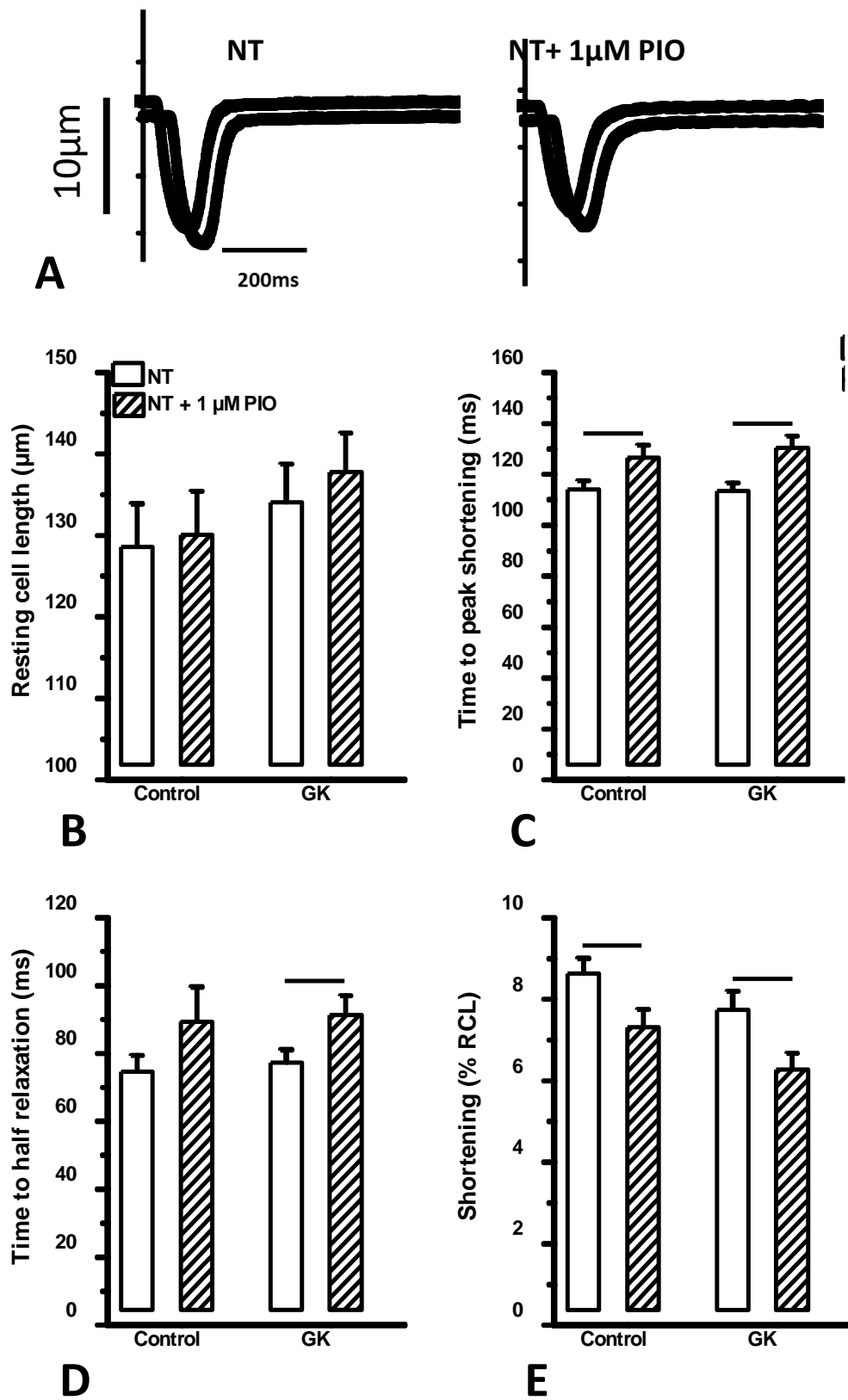


Figure 2

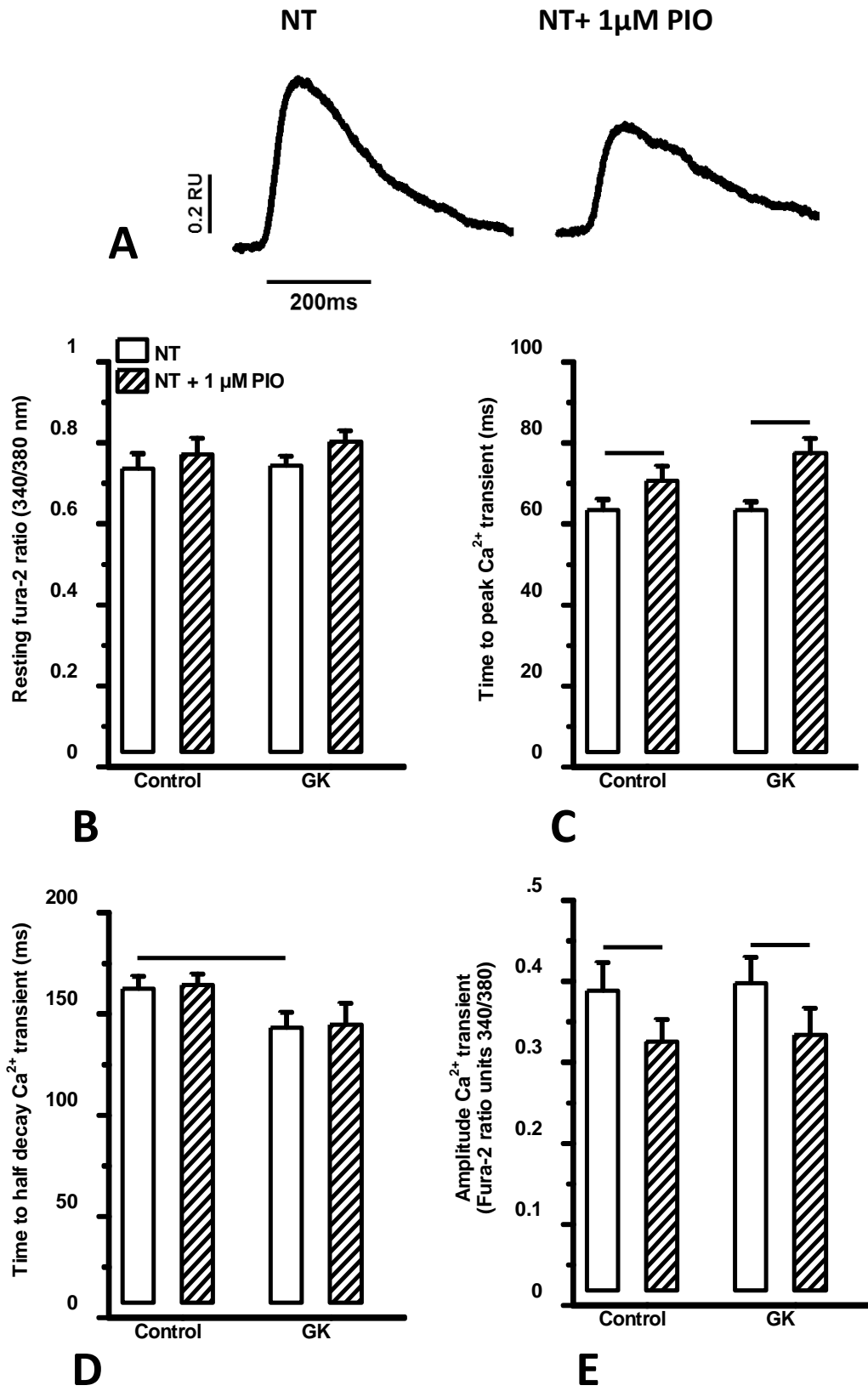
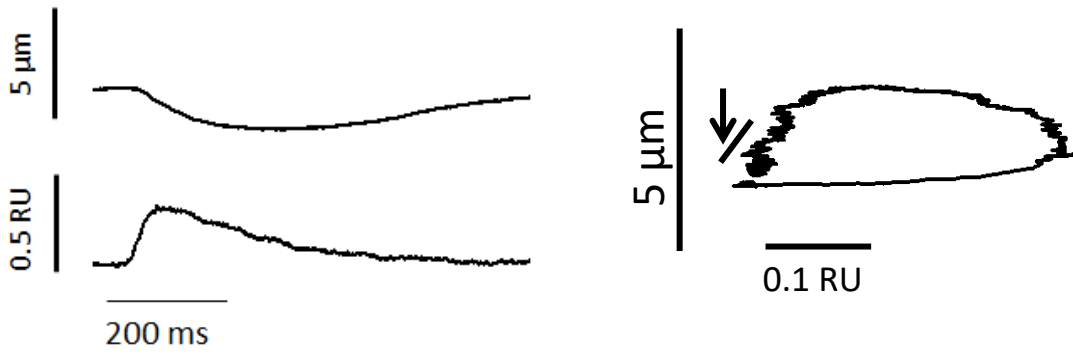
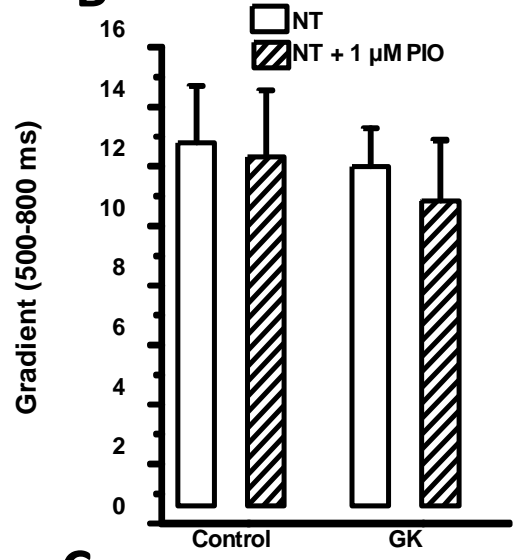


Figure 3

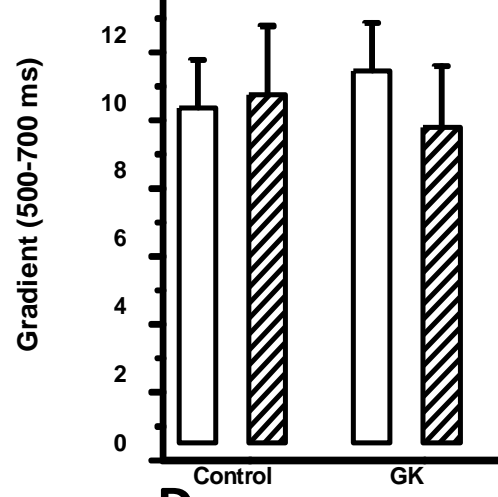


A

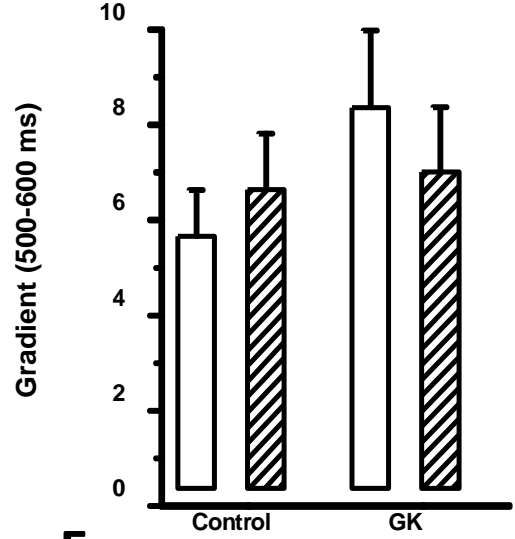
B



D



C



E

Figure 4

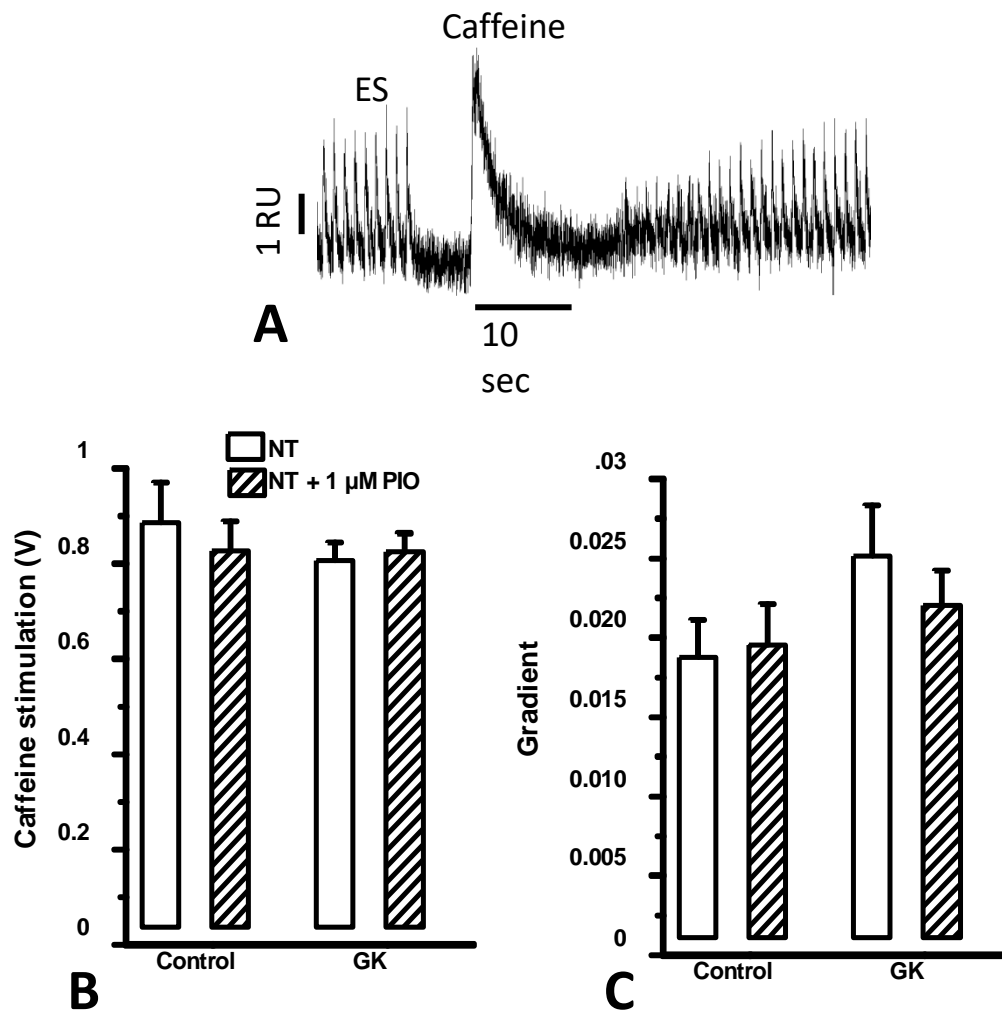
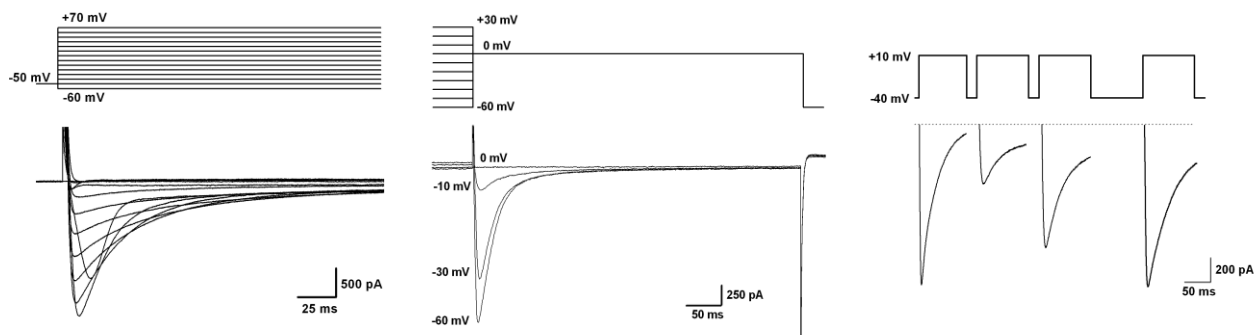


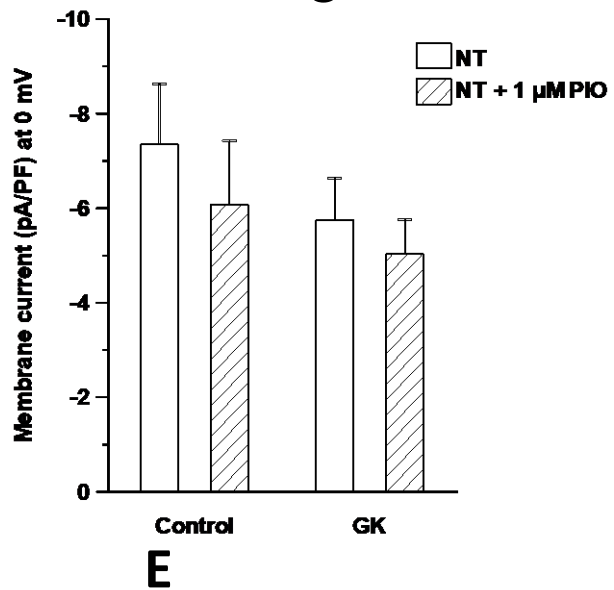
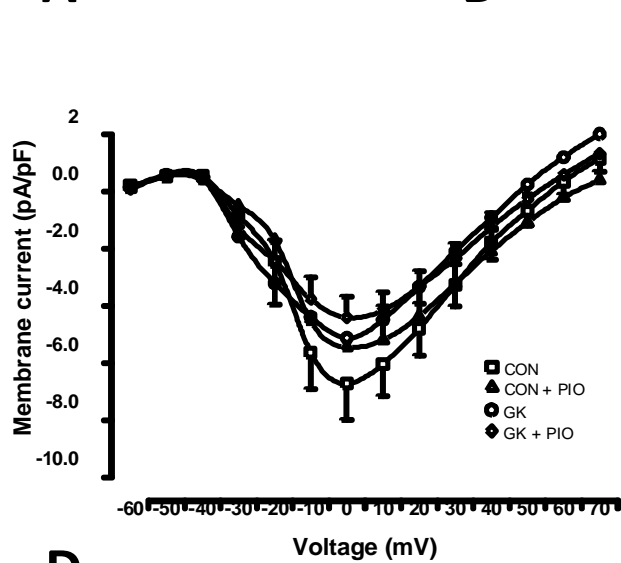
Figure 5



A

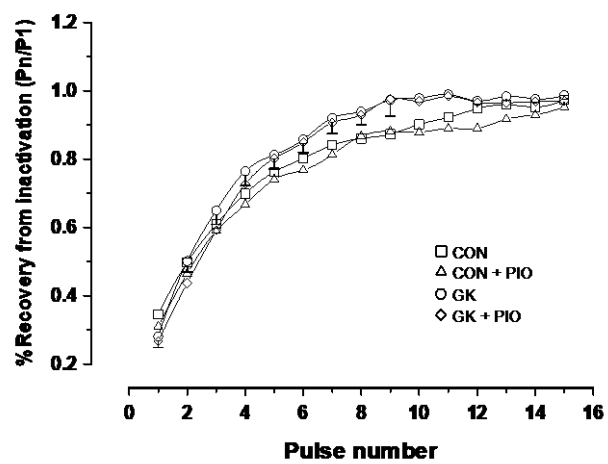
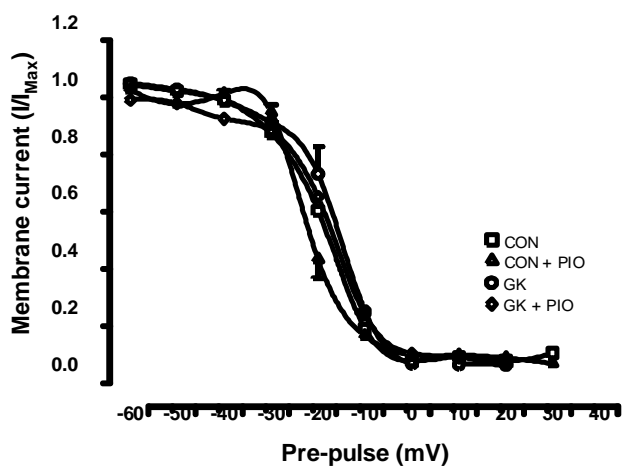
B

C



D

E



F

G

Figure 6